

Charged LFV in a low-scale seesaw mSUGRA model

Amon Ilakovac^a and Apostolos Pilaftsis^b

^aUniversity of Zagreb, Department of Physics, Bijenička cesta 32, P.O.Box 331, Zagreb, Croatia

^bSchool of Physics and Astronomy, Univ. of Manchester, Manchester M13 9PL, United Kingdom

We investigate the influence of the boundary conditions of minimal supergravity (mSUGRA) on the supersymmetric mechanism for lepton flavour violation (LFV) proposed recently [1], within the framework of the MSSM extended by TeV-scale singlet heavy neutrinos. We find that the consideration of the mSUGRA boundary condition may increase the branching ratios of the muon and tauon decaying into three charged leptons by up to a factor of 5, whereas the corresponding branching ratio for their photonic decays remains almost unchanged.

1. SLFV in the MSSM3N

Recently, we proposed [1] a novel, fully supersymmetric mechanism for LFV, which is independent of the soft supersymmetry (SUSY) breaking sector of the theory. The mechanism was called supersymmetric lepton flavour violation (SLFV). To demonstrate the importance of SLFV, we considered a R -parity conserving seesaw extension of the MSSM with one singlet heavy neutrino per family (MSSM3N). The leptonic sector of the superpotential of the MSSM3N reads [1]:

$$W_1 = \hat{E}^C \mathbf{h}_e \hat{H}_d \hat{L} + \hat{N}^C \mathbf{h}_\nu \hat{L} \hat{H}_u + \hat{N}^C \mathbf{m}_M \hat{N}^C \quad (1)$$

where the complex 3×3 matrices, \mathbf{h}_e , \mathbf{h}_ν and \mathbf{m}_M represent the electron and the neutrino Yukawa couplings, and the symmetric heavy neutrino Majorana mass matrix, respectively. We assume that the heavy neutrino sector of the model is $SO(3)$ symmetric being broken down to an $U(1)$ lepton symmetry by the Yukawa sector [2]. The approximate breaking of these symmetries lead to almost degenerate heavy neutrinos, $m_M \approx m_N \mathbf{1}_3$. The approximate flavour symmetries also assure small light neutrino masses, permitting heavy neutrino mass scale as low as 100 GeV, in a way such that the usual see-saw suppression factor of LFV processes, m_ν/m_N is avoided. The SLFV effects depend on the LFV parameters

$$\Omega_{\ell\ell'} = \frac{v_u^2}{2m_N^2} (\mathbf{h}_\nu^\dagger \mathbf{h}_\nu)_{\ell\ell'} \quad (2)$$

In contrast to usual SUSY studies [3] where LFV effects only depend on the flavour structure of the soft SUSY-breaking sector induced by renormalization group (RG) running, SLFV effects only depend on the superpotential heavy neutrino mass scale m_N and the neutrino-Yukawa couplings \mathbf{h}^ν . In addition, they depend on $\langle \sqrt{2} H_u \rangle \equiv v_u = v \cos \beta$, with $v \approx 246$ GeV and $\tan \beta = \langle H_u \rangle / \langle H_d \rangle$.

The SLFV amplitudes are induced by heavy neutrinos and heavy sneutrinos at the one-loop level. The loop sneutrino contributions include heavy sleptons and/or heavy squarks, and therefore they do depend on the soft SUSY-breaking sparticle masses. In Ref. [1], the LFV observables induced by SLFV are evaluated by selecting typical values for the sparticle masses at the electroweak scale. Here, we extend the previous study and evaluate the soft SUSY-breaking parameters, as functions of the heavy neutrino mass scale m_N and the LFV parameters $\Omega_{\ell\ell'}$, using one-loop MSSM3N RG equations [4] with universal boundary conditions at the gauge-coupling unification scale $M_X = 2.5 \times 10^{16}$ GeV. RG analysis confirms that the heavy neutrino sector is supersymmetric almost for the whole parameter space allowed by the perturbative condition on neutrino Yukawa matrices: $\text{Tr}(\mathbf{h}_\nu^\dagger \mathbf{h}_\nu) < 4\pi$. Specifically, the singlet-neutrino sector is supersymmetric to a good approximation, provided the heavy neutrino mass m_N is of comparable or

der or larger than the soft SUSY breaking parameters m_0 (scalar mass), M (gaugino mass) and A_0 (trilinear scalar coupling). In the same kinematic regime, the light left-handed sneutrinos are also degenerate. The superpotential $\hat{H}_u \hat{H}_d$ -mixing term μ turns out to be typically of order 400 GeV, and therefore smaller than the heavy neutrino mass scale m_N , for the largest part of the allowed parameter space. The above justifies the approximations used to obtain the dominant terms of the SLFV amplitudes in Ref. [1].

Within the above framework, we may calculate the leading SLFV amplitudes close to the SUSY limit in the lowest order of v_u and m_N^{-1} . To leading order in g_W and \mathbf{h}_ν , the pertinent LFV amplitudes read [1]:

$$\begin{aligned}\mathcal{T}_\mu^{\gamma l' l} &= \frac{e \alpha_w}{8\pi M_W^2} \bar{l}' \left(F_\gamma^{l' l} q^2 \gamma_\mu P_L \right. \\ &\quad \left. + G_\gamma^{l' l} i \sigma_{\mu\nu} q^\nu m_l P_R \right) l, \\ \mathcal{T}_\mu^{Z l' l} &= \frac{g_w \alpha_w}{8\pi \cos \theta_w} F_Z^{l' l} \bar{l}' \gamma_\mu P_L l, \\ \mathcal{T}_l^{l' l_1 l_2} &= -\frac{\alpha_w^2}{4M_W^2} F_{\text{box}}^{ll' l_1 l_2} \bar{l}' \gamma_\mu P_L l \bar{l}_1 \gamma^\mu P_L l_2,\end{aligned}\quad (3)$$

where $q = p_{\ell'} - p_\ell$. The amplitudes $\mathcal{T}_l^{l' u_1 u_2}$ and $\mathcal{T}_l^{l' d_1 d_2}$ have the same structure as the amplitude $\mathcal{T}_l^{l' l_1 l_2}$, up to replacements $\ell_i \rightarrow u_i \rightarrow d_i$, $i = 1, 2$. The form factors $F_\gamma^{l' l}$, $G_\gamma^{l' l}$, $F_Z^{l' l}$, $F_{\text{box}}^{ll' l_1 l_2}$, $F_{\text{box}}^{ll' u_1 u_2}$ and $F_{\text{box}}^{ll' d_1 d_2}$ receive contributions from both the heavy neutrinos $N_{1,2,3}$ and the right-handed sneutrinos $\tilde{N}_{1,2,3}$. To illustrate the importance of the SLFV effects, we give the leading form of the form factors $F_\gamma^{l' l}$, $G_\gamma^{l' l}$, $F_Z^{l' l}$, $F_{\text{box}}^{ll' l_1 l_2}$, $F_{\text{box}}^{ll' u_1 u_2}$ and $F_{\text{box}}^{ll' d_1 d_2}$ in the Feynman gauge,

$$\begin{aligned}(F_\gamma^{l' l})^N &= \frac{\Omega_{\ell\ell'}}{6 s_\beta^2} \ln \lambda_N, \\ (F_\gamma^{l' l})^{\tilde{N}} &= \frac{\Omega_{\ell\ell'}}{3 s_\beta^2} \sum_{k=1}^2 \nu_{k2}^2 \ln \lambda_{Nk}, \\ (G_\gamma^{l' l})^N &= \Omega_{\ell\ell'} \left(-\frac{1}{6 s_\beta^2} - \frac{5}{6} \right), \\ (G_\gamma^{l' l})^{\tilde{N}} &= \Omega_{\ell\ell'} \left(\frac{1}{6 s_\beta^2} + f \right),\end{aligned}\quad (4)$$

$$(G_\gamma^{l' l})^{\tilde{N}} = \Omega_{\ell\ell'} \left(\frac{1}{6 s_\beta^2} + f \right), \quad (5)$$

$$(F_Z^{l' l})^N = -\frac{3 \Omega_{\ell\ell'}}{2} \ln \lambda_N - \frac{(\Omega_{\ell\ell'}^2)}{2 s_\beta^2} \lambda_N,$$

$$(F_Z^{l' l})^{\tilde{N}} = \Omega_{\ell\ell'} g \ln \lambda_N \quad (6)$$

$$\begin{aligned}F_{\text{box}}^{ll' l_1 l_2} &= -(\delta_{\ell_1 \ell_2} \Omega_{\ell\ell'} + \delta_{\ell' \ell_2} \Omega_{\ell\ell_1}) \\ &\quad + (\Omega_{\ell\ell'} \Omega_{\ell_2 \ell_1} + \Omega_{\ell\ell_1} \Omega_{\ell_2 \ell'}) \frac{\lambda_N}{4 s_\beta^4} \\ F_{\text{box}}^{ll' l_1 l_2} &= (\delta_{\ell_1 \ell_2} \Omega_{\ell\ell'} + \delta_{\ell' \ell_2} \Omega_{\ell\ell_1}) h_\ell \\ &\quad + (\Omega_{\ell\ell'} \Omega_{\ell_2 \ell_1} + \Omega_{\ell\ell_1} \Omega_{\ell_2 \ell'}) \frac{\lambda_N}{4 s_\beta^4}\end{aligned}\quad (7)$$

$$\begin{aligned}F_{\text{box}}^{ll' u_1 u_2} &= 4 \Omega_{\ell\ell'} \\ F_{\text{box}}^{ll' u_1 u_2} &= \Omega_{\ell\ell'} h_u\end{aligned}\quad (8)$$

$$\begin{aligned}F_{\text{box}}^{ll' d_1 d_2} &= -\Omega_{\ell\ell'} \\ F_{\text{box}}^{ll' d_1 d_2} &= \Omega_{\ell\ell'} h_d\end{aligned}\quad (9)$$

where $\lambda_N = \frac{m_N^2}{M_W^2}$, $\lambda_{Nk} = \frac{m_N^2}{m_{\tilde{\chi}_k}^2}$, \mathcal{V} is one of the unitary matrices diagonalizing the chargino mass matrix and f , g , h_ℓ , h_u and h_d are complicated functions of masses and mixing matrices. Detailed results of this study will be given in a forthcoming publication [5].

In the SUSY limit $\tan \beta \rightarrow 1$, $\mu \rightarrow 0$, $m_{\tilde{\chi}_k} \rightarrow M_W$, $f \rightarrow \frac{5}{6}$, $g \rightarrow \frac{3}{2}$, $h_\ell \rightarrow -1$, $h_u \rightarrow 0$ and $h_d \rightarrow -1$. We note that the photonic dipole form factor $G_\gamma^{l' l} = (G_\gamma^{l' l})^N + (G_\gamma^{l' l})^{\tilde{N}}$ vanishes in the SUSY limit. This is a consequence of the SUSY non-renormalization theorem [6]. Beyond the SUSY limit, it strongly depends on the soft SUSY-breaking sector and particularly on the sparticle masses.

In all formfactors, except of $G_\gamma^{l' l}$, the N - and \tilde{N} -loop contributions add constructively. Specifically, in the $M_{\text{SUSY}} \gg M_W$ and in the large M_N limit, the following approximate form factor relations are valid: $F_\gamma^{\ell\ell'} \approx 3(F_\gamma^{\ell\ell'})^N$, $|G_\gamma^{\ell\ell'}| \lesssim |(G_\gamma^{\ell\ell'})^N|$, $F_Z^{\ell\ell'} \approx (F_Z^{\ell\ell'})^N$, $F_{\text{box}}^{ll' l_1 l_2} \approx (F_{\text{box}}^{ll' l_1 l_2})^N$, $F_{\text{box}}^{ll' d_1 d_2} \leq 2(F_{\text{box}}^{ll' d_1 d_2})^N$, and $F_{\text{box}}^{ll' u_1 u_2} \approx (F_{\text{box}}^{ll' u_1 u_2})^N$. It is important to note that the large m_N limit corresponds to a kinematic region where the neutrino Yukawa couplings \mathbf{h}_ν are large (see Eq. (2)). In this limit, the Ω^2 terms dominate in Z and leptonic box amplitudes. More precisely, the terms proportional to Ω^2 become larger than those proportional to Ω , if $g_w^2 < \text{Tr}(\mathbf{h}_\nu^\dagger \mathbf{h}_\nu)$.

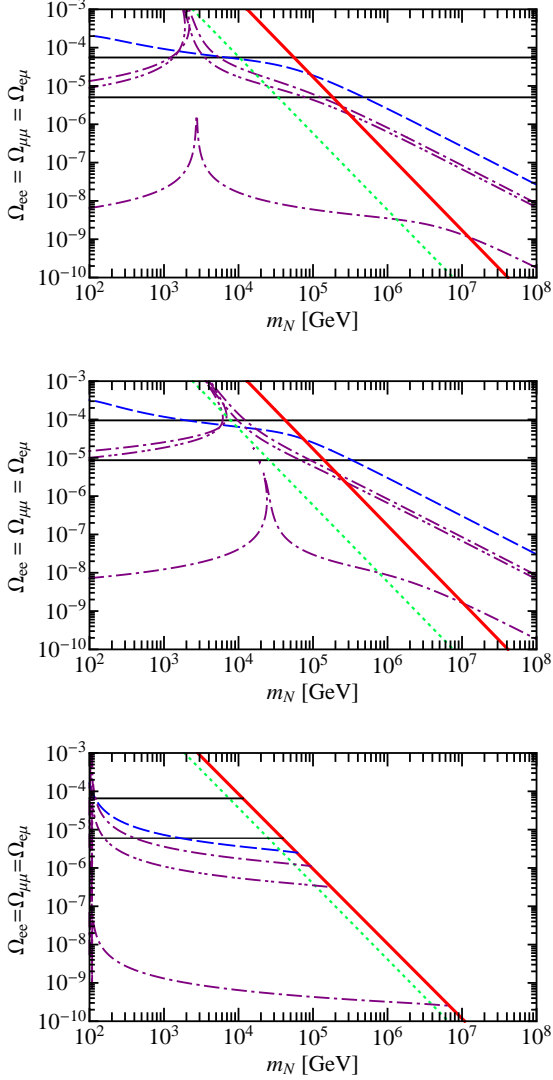


Figure 1. Exclusion contours of $\Omega_{e\mu}$ versus m_N derived from experimental limits on $B(\mu^- \rightarrow e^- \gamma)$ (solid), $B(\mu^- \rightarrow e^- e^- e^+)$ (dashed) and $\mu \rightarrow e$ conversion in Titanium (dash-dotted) and Gold (dash-double-dotted), assuming $\Omega_{ee} = \Omega_{\mu\mu} = \Omega_{e\mu}$ and other $\Omega_{\ell\ell'} = 0$. The upper, middle and lower panel represent the exclusion contours in the SM3N, the MSSM3Nf and the MSSM3NS, respectively. The areas above the contours are excluded; see the text for more details.

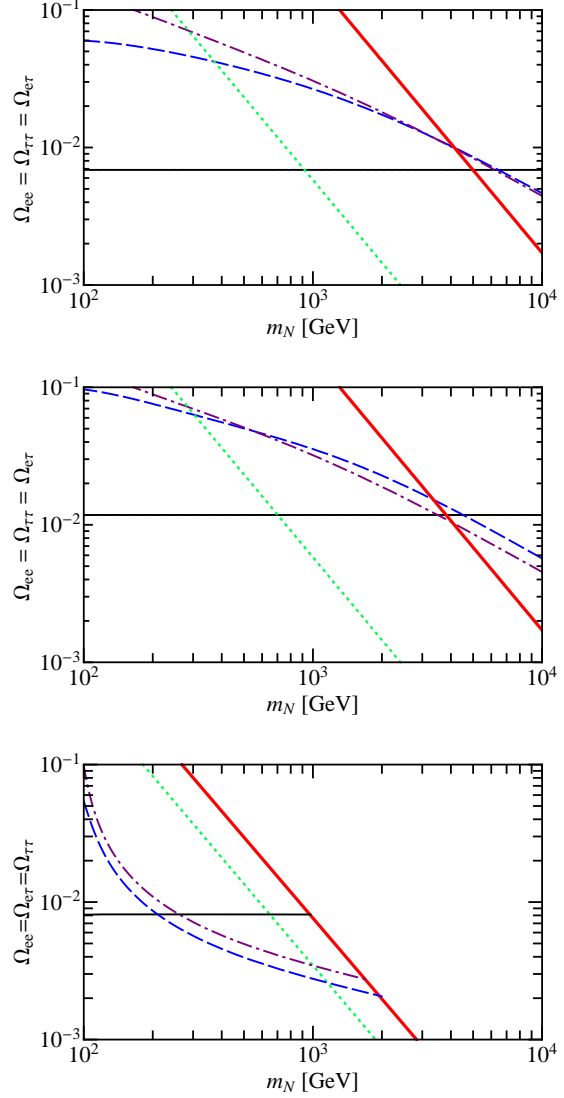


Figure 2. Exclusion contours of $\Omega_{e\tau}$ versus m_N derived from present experimental upper limits on $B(\tau^- \rightarrow e^- \gamma)$ (solid), $B(\tau^- \rightarrow e^- e^- e^+)$ (dashed) and $B(\tau^- \rightarrow e^- \mu^- \mu^+)$ (dash-dotted), assuming that $\Omega_{ee} = \Omega_{\tau\tau} = \Omega_{e\tau}$ and other $\Omega_{\ell\ell'} = 0$. The upper, middle and lower panel represent the exclusion contours in the SM3N, the MSSM3Nf and the MSSM3NS, respectively. The areas above the contours are excluded; more details are given in the text.

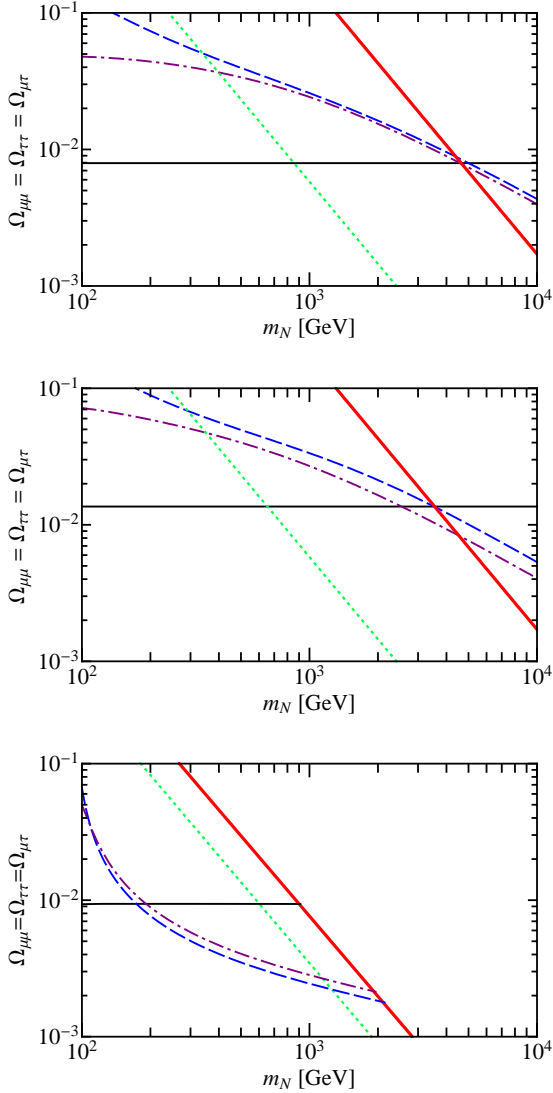


Figure 3. Exclusion contours of $\Omega_{\mu\tau}$ versus m_N derived from present experimental upper limits on $B(\tau^- \rightarrow \mu^- \gamma)$ (solid), $B(\tau^- \rightarrow \mu^- \mu^- \mu^+)$ (dashed) and $B(\tau^- \rightarrow \mu^- e^- e^+)$ (dash-dotted), assuming that $\Omega_{\mu\mu} = \Omega_{\tau\tau} = \Omega_{\mu\tau}$ and other $\Omega_{\ell\ell'} = 0$. The upper, middle and lower panel represent the exclusion contours in the SM3N, the MSSM3Nf and the MSSM3NS, respectively. The areas above the contours are excluded; more details are given in the text.

2. Numerical estimates

We now present numerical estimates of LFV observables in three distinct models: (i) the Standard Model with one heavy right-handed neutrino per family (SM3N); (ii) the MSSM3N with fixed superpartner masses (MSSM3Nf); (iii) the MSSM with mSUGRA boundary conditions (MSSM3NS).

In the SM3N, the LFV amplitudes depend only on $\Omega_{\ell\ell'}$ and m_N . For the SUSY models, the MSSM3Nf and the MSSM3NS, the LFV amplitudes are functions of $\Omega_{\ell\ell'}$, m_N , $\tan\beta$, μ , the slepton and/or squark masses, and the unitary chargino-mixing mass matrices. We take $\tan\beta = 3$, which is a value close to the SUSY limit value $\tan\beta = 1$. In the MSSM3Nf, the lepton and squark matrices and μ are taken as input parameters. We fix $-\mu = \tilde{M}_Q = M_{\tilde{\nu}} = 200$ GeV, $M_{\tilde{W}} = 100$ GeV and $\tan\beta = 3$. In the MSSM3NS, the μ parameter and the sparticle masses are functions of m_N and $\Omega_{\ell\ell'}$. They are determined by the MSSM3N RGEs and the universal soft SUSY-breaking parameters M , m_0 and A_0 defined at the gauge-coupling unification scale M_X . As input values, we take $M = 250$ GeV, $m_0 = 100$ GeV and $A_0 = 150$ GeV.

To simplify our analysis of identifying the regions of parameter space excluded by experimental limits of LFV processes $\mu \rightarrow e + X$ and $\tau \rightarrow e + X$ (where X indicates generically a photon or 3 charged leptons), we consider three separate conservative scenarios with three non-zero $\Omega_{\ell\ell'}$ parameters: $\Omega_{\mu\mu} = \Omega_{\mu e} = \Omega_{ee}$, $\Omega_{\tau\tau} = \Omega_{\tau e} = \Omega_{ee}$, and $\Omega_{\tau\tau} = \Omega_{\tau\mu} = \Omega_{\mu\mu}$ respectively.

The exclusion contours of $\Omega_{e\mu}$ versus m_N for $\mu \rightarrow e + X$ processes, $\Omega_{e\tau}$ versus m_N for $\tau \rightarrow e + X$ and $\Omega_{\mu\tau}$ versus m_N for $\tau \rightarrow \mu + X$ are given in Figs. 1, 2 and 3, respectively. The areas above the curves are forbidden by the experimental upper bounds on the corresponding processes. The area above the diagonal solid lines represent the nonperturbative regime with $\text{Tr}(\mathbf{h}_\nu^\dagger \mathbf{h}_\nu) > 4\pi$, whilst the area above the diagonal dotted lines represent the region where the Yukawa couplings dominate the LFV observables, $\text{Tr}(\mathbf{h}_\nu^\dagger \mathbf{h}_\nu) > g_w^2$. The higher values of $\Omega_{\ell\ell'}$ correspond to smaller values of the LFV observables:

the factors multiplying the combinations of $\Omega_{\ell\ell'}$ elements is smaller, if $\Omega_{\ell\ell'}$ needed to satisfy the experimental upper bound is larger.

The mSUGRA boundary condition has a strong influence on the perturbativity condition: $\text{Tr}(\mathbf{h}_\nu^\dagger \mathbf{h}_\nu) > 4\pi$. In the SM3N and the MSSM3Nf, the condition $\text{Tr}(\mathbf{h}_\nu^\dagger \mathbf{h}_\nu) > 4\pi$ is determined at the M_Z scale. In the MSSM3NS, $\text{Tr}(\mathbf{h}_\nu^\dagger \mathbf{h}_\nu) > 4\pi$ has to be satisfied for any RG scale between M_Z and M_X . As \mathbf{h}_ν increases with the RG scale, the $\text{Tr}(\mathbf{h}_\nu^\dagger \mathbf{h}_\nu) > 4\pi$ is determined at the gauge unification scale, when the typical value for $\text{Tr}(\mathbf{h}_\nu^\dagger \mathbf{h}_\nu)$ at the M_Z scale is $\sim 0.3 - 0.45$. Thus, significant part of the SM3N and MSSM3Nf parameter space in the m_N - $\Omega_{\ell\ell'}$ plane gets excluded in the MSSM3NS. Also, the boundary lines $\text{Tr}(\mathbf{h}_\nu^\dagger \mathbf{h}_\nu) = 4\pi$ and $\text{Tr}(\mathbf{h}_\nu^\dagger \mathbf{h}_\nu) = g_w^2$ come closer to each other. Moreover, the LFV observables cannot be evaluated beyond the perturbativity limit $\text{Tr}(\mathbf{h}_\nu^\dagger \mathbf{h}_\nu) = 4\pi$, since the RGEs rapidly diverge. Instead, in the SM3N and MSSM3Nf, the LFV observables can be computed for any value of m_N and $\Omega_{\ell\ell'}$.

Figures 1, 2 and 3 contain 3 panels. The upper, the middle and the lower panels display exclusion contours obtained in the SM3N, the MSSM3Nf and the MSSM3NS, respectively.

Figure 1 presents exclusion contours for current experimental limits on and future sensitivities to LFV processes of $\mu \rightarrow e$ transitions: $B(\mu^- \rightarrow e^- \gamma) < 1.2 \times 10^{-11}$ [8] (upper horizontal line), $B(\mu^- \rightarrow e^- \gamma) \sim 10^{-13}$ [9] (lower horizontal line), $B(\mu^- \rightarrow e^- e^- e^+) < 10^{-12}$ [8], the constraints from the non-observation of $\mu \rightarrow e$ conversion in ^{48}Ti and ^{197}Au [10], $R_{\mu e}^{\text{Ti}} < 4.3 \times 10^{-12}$ [11] (dash-dotted) and $R_{\mu e}^{\text{Au}} < 7 \times 10^{-13}$ [12] (dash-double-dotted), as well as potential limits from a future sensitivity to $R_{\mu e}^{\text{Ti}}$ at the 10^{-18} level [13] (lower dash-dotted line). Comparing the upper with the middle panel, one can see that $B(\mu \rightarrow e \gamma)$ becomes smaller when the heavy sneutrino contributions are included, while the other observables become larger. The consideration of the mSUGRA boundary condition alter the predictions for the LFV observables in non-trivial manner, i.e. there are no regions of cancelation among terms proportional to Ω and Ω^2 . Furthermore, the theoretical predictions for the LFV observables may increase,

especially for $\mu \rightarrow e$ conversion processes.

Figure 2 exhibits exclusion contours for present experimental limits to LFV processes of $\tau \rightarrow e$ transitions: $B(\tau^- \rightarrow e^- \gamma) < 3.3 \times 10^{-8}$ [15] (solid line), $B(\tau^- \rightarrow e^- e^- e^+) < 2.7 \times 10^{-8}$ [14] (dashed line), and $B(\tau^- \rightarrow e^- \mu^- \mu^+) < 2.7 \times 10^{-8}$ [14] (dash-dotted line). The dominance of the heavy neutrino effects in MSSM3NS manifests already at $m_N \sim 200$ GeV and becomes more pronounced than in the MSSM3Nf. The branching ratios for processes, such as $\tau \rightarrow 3$ leptons, can be ~ 3 times larger than the one for $\tau \rightarrow e \gamma$ at $m_N \sim 1000$ GeV.

Figure 3 exhibits exclusion contours for present experimental limits to LFV processes of $\tau \rightarrow \mu$ transitions: $B(\tau^- \rightarrow \mu^- \gamma) < 4.4 \times 10^{-8}$ [15] (solid line), $B(\tau^- \rightarrow \mu^- \mu^- \mu^+) < 2.1 \times 10^{-8}$ [14] (dashed line), and $B(\tau^- \rightarrow \mu^- e^- e^+) < 1.8 \times 10^{-8}$ [14] (dash-dotted line). The exclusion contours in all three panels are very similar to the corresponding contours for $\tau \rightarrow e$ transitions, but the dominance of the heavy neutrinos is slightly more pronounced. In particular, the heavy neutrino dominance in the MSSM3NS manifests before $m_N \sim 200$ GeV and $B(\tau \rightarrow 3 \text{ leptons})$ can be about 5 times larger than $B(\tau \rightarrow \mu \gamma)$ at $m_N \sim 1000$ GeV.

In summary, we have shown that the incorporation of the mSUGRA boundary condition into the MSSM3N leads to larger theoretical predictions for the LFV observables $R_{\mu e}$, $\mu \rightarrow 3e$ and $\tau \rightarrow 3$ leptons by up to a factor of 5. The branching ratios for the $\ell \rightarrow \ell' \gamma$ processes show a smaller variation; they are slightly larger than those obtained in the MSSM3Nf but smaller than the ones in the SM3N. We plan to present detailed results of this preliminary analysis in the near future [5].

Acknowledgements: A.I. thanks K. Kumerički and L. Popov for some programming help. The work of A.I. was supported by Ministry of Science, Sports and Technology under contract 119-0982930-1016, and the work of A.P. in part by the STFC research grant: PP/D000157/1.

REFERENCES

1. A. Ilakovac and A. Pilaftsis, Phys. Rev. D **80** (2009) 091902.
2. A. Pilaftsis, Phys. Rev. Lett. **95** (2005) 081602; A. Pilaftsis and T.E.J. Underwood, Phys. Rev. D **72** (2005) 113001.
3. F. Borzumati and A. Masiero, Phys. Rev. Lett. **57** (1986) 961; J. Hisano, T. Moroi, K. Tobe and M. Yamaguchi, Phys. Rev. D **53** (1996) 2442.
4. P.H. Chankowski and S. Pokorski, Int. J. Mod. Phys. A **17** (2002) 575; S.T. Petcov et al., Nucl. Phys. B **676** (2004) 453.
5. A. Ilakovac, A. Pilaftsis and L. Popov in preparation.
6. S. Ferrara and E. Remiddi, Phys. Lett. B **53** (1974) 347.
7. H. C. Chiang, E. Oset, T. S. Kosmas, A. Faessler and J. D. Vergados, Nucl. Phys. A **559** (1993) 526.
8. C. Amsler *et al.*, Phys. Lett. B **667** (2008) 1.
9. S. Ritt [MEG Collaboration], Nucl. Phys. Proc. Suppl. **162** (2006) 279.
10. To get predictions for $R_{\mu e}$, we use the values for $Z_{eff} |F(-m_\mu^2)|$ and Γ_{capt} given by R. Kitano, M. Koike and Y. Okada, Phys. Rev. D **66** (2002) 096002.
11. SINDRUM II collaboration, C. Dohmen *et al.*, Phys. Lett. B **317** (1993) 631.
12. W. Bertl *et al.*, Eur. Phys. J. C **47** (2006) 337.
13. Y. Kuno, Nucl. Phys. Proc. Suppl. **149** (2005) 376.
14. K. Hayasaka et al., Belle Collaboration, Phys. Lett. B **687** (2010) 139.
15. B. Aubert et al. Babar Collaboration, Phys. Rev. Lett. **104** (2010) 021802.